Current-Recycling Complex Filter for Bluetooth-Low-Energy Applications

Anith Selvakumar and Antonio Liscidini, *Senior Member, IEEE*

***Abstract*—This brief presents a flexible gm-C complex filter for Bluetooth-low-energy receivers. Each complex pole is realized sharing a bias current among transconductors, leading to an ultralow-power solution. The filter, which is designed in the 130-nm complimentary metal–oxide–semiconductor technology, has a power dissipation of only 42 μW from a 0.8-V supply voltage. With a center frequency and a passband of 2 and 1 MHz, respectively, the simulated filter provides a rejection of the adjacent channel of 34 dB and a spurious-free dynamic range of 52.7 dB.**

***Index Terms*—Bluetooth low energy (BLE), complex filter, complimentary metal–oxide–semiconductor (CMOS), gm-C, low power, low voltage, wireless receiver, wireless sensor network.**

I. Introduction

BLUETOOTH low energy (BLE) is a new operative mode introduced in the fourth release of the Bluetooth wireless technology standard. BLE is tailored toward ultralow-power devices powered by coin cell batteries, such as wireless sensor networks for indoor localization, wireless payment tags, and wearable devices [1]. In such applications, performance can be sacrificed in favor of an extended battery life obtained by minimizing the overall power consumption of the radio.

In the design of the analog baseband of a radio, current-recycling approaches can lead to a significant reduction in the power dissipation. An example is the very clever solution proposed by Lin *et al.*, where a complex pole is synthesized sharing the same current among all the transconductors of the gm-C cell [2]. The price for its compact and simple structure is a lack of flexibility since, as it will be shown in this brief, such kind of cell only allows the synthesis of complex poles where the real part is larger than the imaginary part. This results in a constraint on the maximum frequency shift of the resulting bandpass filter. The aim of this brief is to remove this limitation by modifying the topology to allow the synthesis of any complex pole while preserving the low-power characteristics of the original structure.

This brief is structured as follows. In Section II, the original topology proposed by Lin *et al.*, is analyzed, showing that a stability issue limits the possible pole configurations. In Section III, the topology is modified in order to obtain unconditional stability for any kind of complex pole. Finally, a design based on the proposed topology is presented in Section IV.

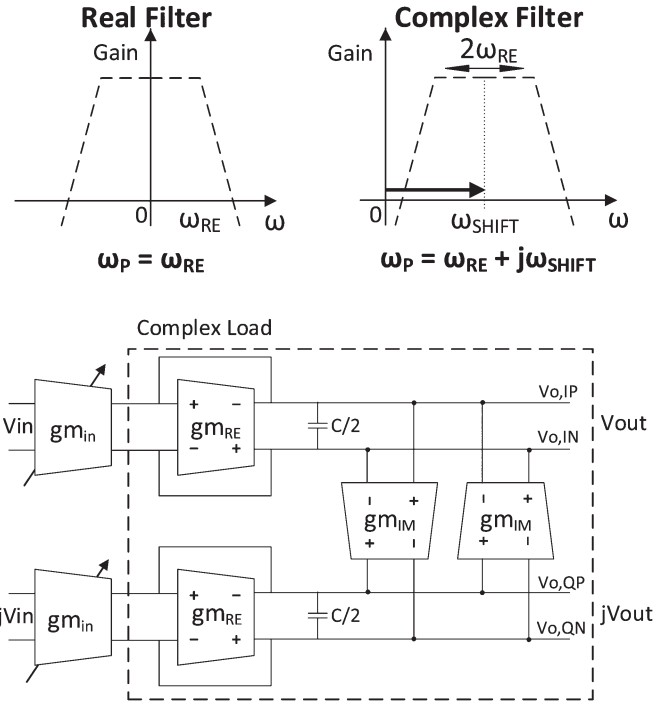

Fig. 1. Complex pole and typical gm-C implementation.

II. Current Reuse Complex Filter

In low-IF receivers, channel selection and image rejection can be performed by a complex filter at the baseband frequency [3]. Complex poles are implemented by shifting the real poles of a low-pass filter to form a bandpass response (see Fig. 1). In gm-C filters, the complex pole is obtained adopting the block diagram in Fig. 1. The real component of the pole is synthesized through transconductances $gm_{\rm RE}$ in shunt with capacitance C having

$$\omega_{3\ \rm dB} = \frac{gm_{\rm RE}}{C} \tag{1}$$

whereas for the imaginary part, transconductances $gm_{\rm IM}$ with cross-connected I and Q paths are used. The frequency shift is proportional to $gm_{\rm IM}$ and is given by

$$\omega_{\rm shift} = \frac{gm_{\rm IM}}{C}. \tag{2}$$

Manuscript received July 27, 2014; revised September 30, 2014; accepted November 29, 2014. Date of publication January 6, 2015; date of current version April 1, 2015. This brief was recommended by Associate Editor M. Onabajo.

The authors are with the Edward S. Roger Sr. Department of Electrical & Computer Engineering, University of Toronto, Toronto, ON M5S 3G4, Canada (e-mail: a.selvakumarasingam@mail.utoronto.ca; antonio.liscidini@utoronto.ca).

Color versions of one or more of the figures in this brief are available online at http://ieeexplore.ieee.org.

Digital Object Identifier 10.1109/TCSII.2014.2387611

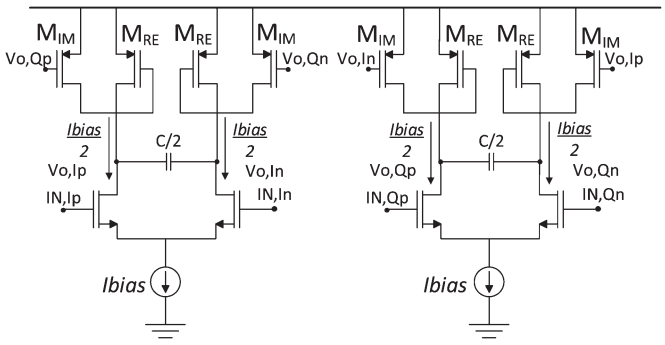

Fig. 2. Current-recycling complex filter.

These two components combined lead to the complex pole as

$$\omega_{\mathrm{COMPLEX}} = \frac{gm_{\mathrm{RE}}}{C} + \frac{gm_{\mathrm{IM}}}{C} = \omega_{3\ \mathrm{dB}} + j\omega_{\mathrm{shift}}. \quad (3)$$

Notice that, in order to have a bandpass transfer function in the positive frequency domain, ω_{shift} must be greater than $\omega_{3\ \mathrm{dB}}$. The ratio between these two quantities can also define a sort of quality factor for the bandpass filter, which can be expressed as

$$Q = \frac{\omega_{\mathrm{shift}}}{\omega_{3\ \mathrm{dB}}} = \frac{gm_{\mathrm{IM}}}{gm_{\mathrm{RE}}}. \quad (4)$$

As shown by (4), the gm-C filter's quality factor just depends on the ratio between gm_{IM} and gm_{RE}. In addition, a bandpass transfer function can be only obtained if $Q > 1$ (i.e., $gm_{\mathrm{IM}} > gm_{\mathrm{RE}}$).

A. Current Reuse Topology

In order to save power, Lin *et al.*, have proposed the solution reported in Fig. 2, where the bias current is recycled among the transconductance stages [2]. In this topology, the bias current of input transconductor gm_{IN} is reused to implement both gm_{RE} and gm_{IM}. $\mathrm{M_{IM}}$ and $\mathrm{M_{RE}}$ can be sized according to the frequency shift and bandwidth desired by the designer.

Unfortunately, the solution proposed by Lin *et al.*, has an intrinsic limit in the achievable ratio Q between the frequency shift and the filter bandwidth. This limit is due to a stability issue that will be now analyzed.

B. Pole Position and Filter Stability

All differential complex filters designed according to the scheme in Fig. 1 have an intrinsic positive common-mode feedback loop that is maintained stable by adopting fully differential transconductors with an adequate common-mode rejection ratio [4]. The solution proposed by Lin *et al.*, in Fig. 2 uses a pseudodifferential architecture for transconductors gm_{RE} and gm_{IM}; thus, it is unable to reject the common-mode signals. This choice sets a severe constraint in the design of the complex pole to avoid instability.

Analyzing the structure in Fig. 2, it is possible to verify that the cascade of transconductances gm_{RE} and gm_{IM} creates the positive feedback loop shown in Fig. 3. The positive loop is formed by the four common-source amplifier stages $\mathrm{M_{IM}}$ loaded by the diode-connected transistor $\mathrm{M_{RE}}$. It can be easily

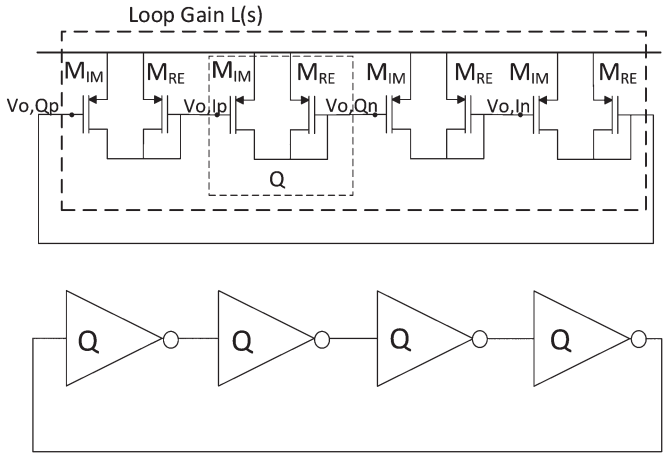

Fig. 3. Positive feedback loop limits the shift that can be implemented under this topology.

seen that the gain of each stage is equal to Q, whereas the overall loop gain is equal to

$$L(s) = Q^4 = \left(\frac{gm_{\mathrm{IM}}}{gm_{\mathrm{RE}}}\right)^4. \quad (5)$$

Since the stability of this positive loop is only guaranteed when $|L(s)| \leq 1$, Q must be lower than one, and consequently, we have

$$gm_{\mathrm{IM}} \leq gm_{\mathrm{RE}}. \quad (6)$$

Since gm_{IM} cannot exceed gm_{RE}, frequency shift ω_{shift} must be lower than the filter bandwidth preventing the synthesis of a bandpass filter. This constraint can particularly become an issue in low-IF receivers, where flicker noise can corrupt the signal band unless a sufficiently high IF is chosen. An example is the channel selection filter for a Bluetooth receiver generally centered at 2 MHz with a bandwidth of 1 MHz [5]. In the next section, it will be shown how to modify the filter proposed by Lin *et al.*, in order to maintain ultralow-power capabilities but avoid the latching of the structure due to a loop gain that is greater than 1.

III. Proposed Current-Recycling Complex Filter

In order to safely synthesize any complex pole without violating stability conditions, the original topology proposed by Lin *et al.*, was modified, introducing an additional cross-coupled pair, as shown in Fig. 4. The key idea is to add an additional degree of freedom by having a common-mode gain that differs from the differential gain.

For the common-mode signal, the cross-coupled transistors act as an additional transconductance in parallel to gm_{RE} that reduces the common-mode gain of the stage (and with it, the positive loop gain). On the contrary, for the differential signal, the cross-coupled transistor behaves as a negative resistance that, combined with $\mathrm{M_{RE}}$, defines the bandwidth of the filter (i.e., $\omega_{3\ \mathrm{dB}}$).

Contrary to the original complex gm-C cell, with this new topology, there exist an infinite number of combinations that can be used to synthesize any kind of ratio Q while preserving

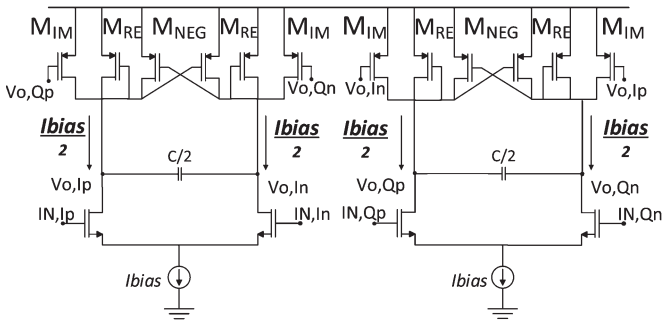

Fig. 4. Proposed current-recycling complex filter.

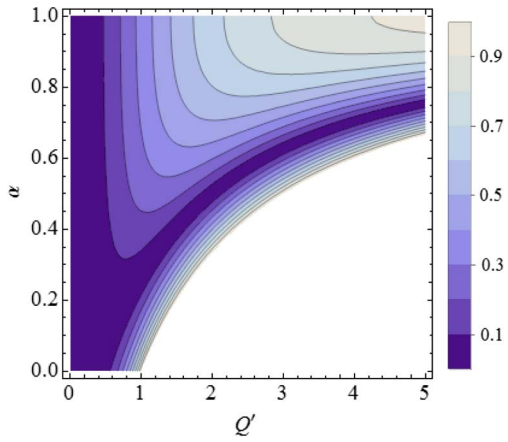

Fig. 5. Contour plot showing the set of possible α and Q', where the positive feedback loop is stable.

the stability. Furthermore, since no additional transistors were stacked to reject the common-mode signals, the same voltage supply of the original scheme can be preserved, maintaining all the benefits of the original current-recycling technique.

A. Differential Signal Transfer Function

For differential signals, the cross coupling of transistor M_{NEG} creates a negative conductance in parallel to the diode-connected transistor M_{RE}, leading to an effective transconductance equal to

$$gm_{\mathrm{RE(eff)}} = gm_{\mathrm{RE}} - gm_{\mathrm{NEG}}. \tag{7}$$

The reduction of transconductance gm_{RE} results in a new location of the complex pole given by

$$\omega'_{\mathrm{COMPLEX}} = \frac{gm_{\mathrm{RE(eff)}}}{C} + j\frac{gm_{\mathrm{IM}}}{C} \tag{8a}$$

$$= \frac{(gm_{\mathrm{RE}} - gm_{\mathrm{NEG}})}{C} + j\frac{gm_{\mathrm{IM}}}{C} \tag{8b}$$

$$= \omega_{3\ \mathrm{dB}} + j\omega_{\mathrm{shift}}. \tag{8c}$$

The filter bandwidth is now determined by $gm_{\mathrm{RE(eff)}}$ (i.e., the difference between transconductances gm_{RE} and gm_{NEG}). The new ratio Q' can be written as

$$Q' = \frac{gm_{\mathrm{IM}}}{gm_{\mathrm{RE(eff)}}} = \frac{gm_{\mathrm{IM}}}{gm_{\mathrm{RE}} - gm_{\mathrm{NEG}}}. \tag{9}$$

Notice that the effect of the negative transconductance is to increase the quality factor of the filter, as a negative resistance would do when placed in parallel to an LC bandpass filter.

B. Common-Mode Loop Gain

For the common-mode signals, as the cross-coupled transistors no longer act like a negative conductance, the gain of each stage differs from (9); thus, $L(s)$ is no longer equal to Q^4. The new expression of the loop gain is given by (10), as shown at the bottom of the page. Once again, the positive feedback loop described by (10) reaches instability when $L(s) > 1$. However, in this case, this occurs when

$$gm_{\mathrm{IM}} = gm_{\mathrm{RE}} + gm_{\mathrm{NEG}}. \tag{11}$$

If the gain of each stage is not equal to 1, M_{NEG} experiences an attenuation or boost of its transconductance (gm_{NEG}) proportional to the gain across the transistor.

C. Stability Conditions

The relation between the stability and the complex pole position can be studied by rewriting (10) as a function of Q' and a new parameter α, which is defined as the ratio between the negative and positive transconductances (i.e., $\alpha = gm_{\mathrm{NEG}}/gm_{\mathrm{RE}}$), as

$$L(Q', \alpha) = \frac{Q'^4(\alpha - 1)^2 - 2Q'^2\alpha}{1 + \alpha(2 + 2Q'^2 + \alpha)}. \tag{12}$$

The contour plot of (12) drawn in Fig. 5 clearly shows all the possible sets (α, Q') that yield $L < 1$. A higher stability margin is obtained by choosing α in the darker areas. To avoid the possibility of instability in case α excessively varies under process, voltage, and temperature, α should be also chosen around regions of gradual variation in the loop gain. The plot also shows that, when no negative transconductance is used (i.e., $\alpha = 0$), as in the original solution proposed by Lin *et al.*, the stability can be only guaranteed for $Q' < 1$ [3].

The negative transconductance used to avoid the stability issues introduces an additional source of noise at the output of the stage. However, this noise has no significant impact on the overall noise performance of the filter, being generally dominated by the noise of the input stage (particularly when a high-voltage gain is designed for the cell). Furthermore, as the negative transconductance is placed in parallel to the complex

$$L(s)|_{\mathrm{DC}} = \frac{gm_{\mathrm{IM}}^4 - 2gm_{\mathrm{IM}}^2 gm_{\mathrm{RE}} gm_{\mathrm{NEG}}}{gm_{\mathrm{IM}}^4 + 2gm_{\mathrm{IM}}^2 gm_{\mathrm{RE}} gm_{\mathrm{NEG}} - 2gm_{\mathrm{RE}}^2 gm_{\mathrm{NEG}}^2 + gm_{\mathrm{NEG}}^4} \tag{10}$$

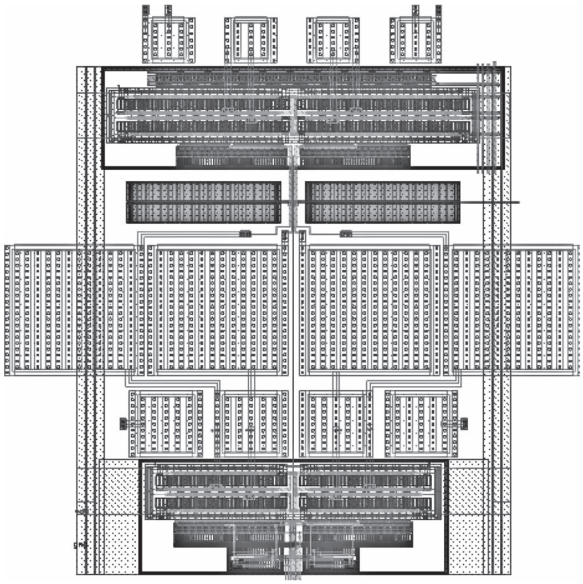

Fig. 6. Complex filter layout in the IBM 130-nm CMOS technology.

load, there is no additional headroom voltage loss from the original solution proposed by Lin *et al.* Specifically, the upper bound on the voltage swing is only limited by one voltage overdrive to achieve the same linearity as the original topology.

IV. Circuit Implementation

The proposed topology in Fig. 4 was used to realize a second-order complex biquad filter centered at 2 MHz and with a bandwidth of 1 MHz suitable for BLE applications. The filter was designed with the 130-nm complimentary metal–oxide–semiconductor (CMOS) technology provided by IBM under a reduced voltage supply of 0.8 V (see Fig. 6). Its low supply voltage makes the filter suitable for wireless autonomous devices, taking advantage of energy harvesting technologies, such as photovoltaic cells, where the voltage supply generated is typically less than 1 V. [6]

The complex pole was synthesized using (8a) to determine the effective transconductances and capacitances required, noting that a 500-kHz baseband pole frequency shifted to 2 MHz, for example, would result in a 1-MHz passband. The effective real transconductance, i.e., $gm_{\mathrm{RE(eff)}}$, can be then decomposed into the diode-connected and cross-coupled transistors through a ratio determined from the contour stability plot in Fig. 5. For the second-order filter implemented, two complex poles (with two different frequency shifts) were synthesized and cascaded in order to realize the flatband response shown in Fig. 7, with a center frequency of 2 MHz. For the first pole, a quality factor of 4.7 required that the ratio of negative-to-positive transconductances, i.e., α, be between 0.6 and 1 in order to achieve a stable loop. For the highest gain margin, α was selected to be 0.7, resulting in $\mathrm{M_{RE}}$ and $\mathrm{M_{NEG}}$ sizes of $W = 50\ \mu\mathrm{m}$ and $W = 35\ \mu\mathrm{m}$, respectively, with $L = 1.5\ \mu\mathrm{m}$. Based on the desired frequency shift, $\mathrm{M_{IM}}$ was sized with $W = 70\ \mu\mathrm{m}$ and having a similar length as $\mathrm{M_{RE}}$ and $\mathrm{M_{NEG}}$. The second pole was implemented in a similar manner according to the quality factor of 6.7. Table I shows the performance summary achieved, along with a comparison with similar complex filter implementations suitable for BLE.

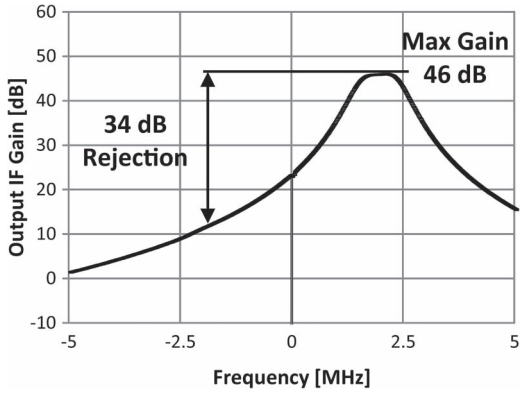

Fig. 7. IF gain profile for the complex filter implemented.

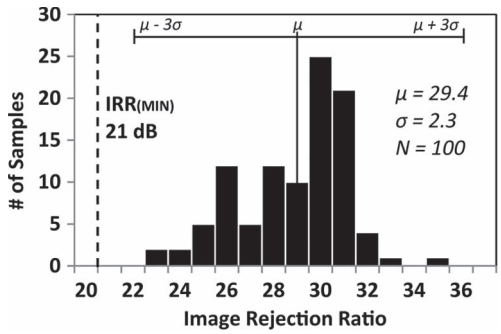

Fig. 8. IRR under both mismatch and process variations.

A. Simulation Results

The simulation results of the proposed filter only show 42-μW power consumption while providing a maximum gain of 46-dB in-band gain and 34 dB of adjacent channel suppression.

Overall, the performance was evaluated by the spurious-free dynamic range (SFDR), which is the difference between the minimum detectable signal at the output and the maximum power of an out-of-band blocker to produce intermodulation products in-band equal to the integrated noise of the filter [also known as the third-order input intercept point (IIP3)] [7]. The simulation results yield an SFDR of 52.7 dB for out-of-band signals, with an IIP3 of -12 dBm and an integrated input-referred noise of 5.7 $\mu\mathrm{V_{rms}}$. To obtain this measurement, two out-of-band tones were placed at 5 and 8 MHz in order to have an in-band intermodulation product at 2 MHz. This scenario corresponds to the interferers from adjacent channels in BLE that can produce the unwanted tone. The filter performance under both the device mismatch and random process variations was obtained through Monte Carlo simulations and is shown in Fig. 8. The results from 100 iterations yield a mean image rejection ratio (IRR) of 29.4 with a standard deviation of 2.3, demonstrating full compliance to BLE's IRR requirement (> 21 dB) within three standard deviations of the expected value. Any unwanted shifts in the transfer function due to process,

TABLE I
COMPLEX FILTER PERFORMANCE SUMMARY

	[9]	[10]	[11]	[12]	[13]	**This Work**
Topology	*Gm-C*	*CA-RC*	*Gm-C*	*Current Mirror*	*Current Mirror*	***Gm-C***
Order	3	4	5	6	6	**2**
Bandwidth [MHz]	2	1	1.170	0.9	1	**1**
Frequency Shift [MHz]	2	3	0.995	2	1	**2**
Adjacent Channel Rejection [dB]	35	-	48	28	49	**34**
Max Gain [dB]	-	-	18.4	-	-	**46**
Integrated In-Band IRN [uV]	-	73	50.4	1215	-	**5.7**
SFDR[dB]	55.5	77.8	70	53.8	56.3	**52.7**
Power Diss [uW]	1200	1000	640	4710	3200	**42**
Area [mm^2]	-	0.4	0.15	-	-	**0.12**
Vdd [V]	1.2	1.8	1.2	1.5	1.5	**0.8**
Technology [nm]	90	180	180	350	350	**130**
FoM (fJ)	0.50	0.001	0.01	1.6	1.1	**0.05**

temperature, and supply voltage variations can be easily corrected by adjusting the bias current to recalibrate the filter response.

The following figure of merit (FoM) was used in order to evaluate the performance of this design against similar filters proposed in literature:

$$\text{Figure of Merit} = \frac{\text{Power Consumption}}{(\#\text{Poles})\left(\sqrt{f_c^2 + \frac{f_{BW}^2}{2}}\right)(\text{SFDR})}.$$

The FoM is based on that in [8] but revised to take into account both the frequency shift and the bandwidth of the complex filter.

Among the complex filters in the presented recent literature, the proposed design achieves a performance comparable with the current state of the art but using a lower voltage supply. With the exception of the CA-RC filter presented in [10], the gm-C structure yields higher performance than the current mirror designs in [12] and [13], providing higher channel rejection while consuming less power and requiring a fewer number of stages. The proposed high-performance low-power gm-C filter presented in this brief achieves a FoM of 0.05 fJ, with power consumption that is only a fraction of the current state of the art.

V. CONCLUSION

In this brief, a gm-C complex filter cell for a low-power application has been presented. The proposed solution derives from an idea presented by Lin *et al.*, where the bias current is recycled among the transconductances used to implement the gm-C stage. In the original topology, a stability issue limits the possible complex poles synthesizable. The proposed approach solved the problem by adding a negative transconductance at the output of the stage in order to achieve a common-mode gain different from the differential gain. This results in the flexibility to synthesize any complex pole with no restriction on the maximum shift. To demonstrate this, a stable second-order biquad filter of a 1-MHz bandwidth and a 2-MHz center frequency was implemented for the BLE wireless standard and presented in this brief.

REFERENCES

[1] J. Masuch and M. Delgado-Restituto, "A 1.1-mW-RX −81.4 dBm sensitivity CMOS transceiver for Bluetooth low energy," *IEEE Trans. Microw. Theory Techn.*, vol. 61, no. 4, pp. 1660–1673, Apr. 2013.

[2] Z. Lin, P. Mak, and R. Martins, "A 1.7 mW 0.22 mm^2 2.4 GHz ZigBee RX exploiting a current-reuse blixer and hybrid filter topology in 65 nm CMOS," in *Proc. IEEE Int. Solid-State Circuits Conf. Dig. Tech. Papers*, Feb. 2013, pp. 448–449.

[3] J. Crold and M. Steyaert, *CMOS Wireless Transceiver Design*. Boston, MA, USA: Kluwer, 1997.

[4] A. Emira and E. Sanchez-Sinencio, "A pseudo differential complex filter for Bluetooth with frequency tuning," *IEEE Trans. Circuits Syst. II, Analog Digit. Signal Process.*, vol. CAS2-50, no. 10, pp. 742–754, Oct. 2003.

[5] *Bluetooth Specification Version 4.1*. [Online]. Available: http://www.bluetooth.com

[6] M. Danesh and J. R. Long, "Photovoltaic antennas for autonomous wireless systems," *IEEE Trans. Circuits Syst. II, Exp. Briefs*, vol. 58, no. 12, pp. 807–812, Dec. 2011.

[7] B. Razavi, *RF Microelectronics*, 2nd ed. New York, NY, USA: Castleton, 2011.

[8] A. Yoshizawa and Y. P. Tsividis, "Anti-blocker design techniques for MOSFET-C filters for direct conversion receivers," *IEEE J. Solid-State Circuits*, vol. 37, no. 3, pp. 357–364, Mar. 2002.

[9] M. Tedeschi, A. Liscidini, and R. Castello, "Low-power quadrature receivers for ZigBee (IEEE 802.15.4) applications," *IEEE J. Solid-State Circuits*, vol. 45, no. 9, pp. 1710–1719, Sep. 2010

[10] H. A. Alzaher, N. Tasadduq, and F. S. Al-Ammari, "Optimal low power complex filters," *IEEE Trans. Circuits Syst. I, Reg. Papers*, vol. 60, no. 4, pp. 885–895, Apr. 2013.

[11] B. Guthrie, J. Hughes, T. Sayers, and A. Spencer, "A CMOS gyrator low-IF filter for a dual-mode Bluetooth/ZigBee transceiver," *IEEE J. Solid-State Circuits*, vol. 40, no. 9, pp. 1872–1879, Sep. 2005.

[12] C. Laoudias and C. Psychalinos, "1.5-V complex filters using current mirrors," *IEEE Trans. Circuits Syst. II, Exp. Briefs*, vol. 58, no. 9, Sep. 2011.

[13] C. Laoudias and C. Psychalinos, "Low-voltage Bluetooth/ZigBee complex filter using current mirrors," in *Proc. IEEE ISCAS*, Paris, France, May 2010, pp. 1268–1271.